Tensor correlations and evolution of single-particle energies in medium-mass nuclei

Wei Zou,[1,2,3] Gianluca Colò,[1] Zhongyu Ma,[2] Hiroyuki Sagawa,[4] and Pier Francesco Bortignon[1]
[1]*Dipartimento di Fisica, Università degli Studi and INFN, Sezione di Milano, via Celoria 16, I-20133 Milano, Italy*
[2]*China Institute of Atomic Energy (CIAE), Beijing 102413, People's Republic of China*
[3]*Physics Department, Jilin University, Changchun 130012, People's Republic of China*
[4]*Center for Mathematical Sciences, University of Aizu, Aizu-Wakamatsu, Fukushima 965-8560, Japan*
(Received 26 September 2007; published 22 January 2008)

We analyze the evolution of the spin-orbit splittings in the Ca isotopes and in the $N = 28$ isotones. We also focus on the reduction of the spin-orbit splittings associated with f and p orbits from ^{48}Ca to ^{46}Ar. We conclude that adding the tensor contribution can qualitatively explain in most cases the empirical trends, whereas this is not the case if one simply employs existing Skyrme parametrizations without the tensor force.

DOI: 10.1103/PhysRevC.77.014314 PACS number(s): 21.30.Fe, 21.10.Dr, 21.10.Pc, 21.60.Jz

I. INTRODUCTION

The effective zero-range interaction proposed by Skyrme in the 1950s [1], and named later after him, includes a tensor component. However, this component was neglected when realistic Skyrme parameter sets have been determined in the 1970s [2]. Afterwards, there were few works on the tensor component of the Skyrme force and these works did not allow a definite, positive global statement about the relevance of the tensor component. In the study of Stancu, Brink, and Flocard [3], who added the tensor force perturbatively to the SIII parametrization, it was pointed out that some spin-orbit splittings in magic nuclei can be improved with a tensor force, but the improvements are considered "minor" by the authors themselves. A complete fit of the Skyrme parameters which includes the terms from the tensor force in spherical nuclei, was done by Tondeur [4], i.e., the spin-orbit and tensor terms of the force were constrained by selected spin-orbit splittings in ^{16}O, ^{48}Ca, and ^{208}Pb. The results for the masses and density distributions are satisfactory but there is no detailed consideration about the single-particle states. Analogously, the issue of single-particle states was not specifically addressed in Ref. [5], in which the Skyrme parameters were fitted by including the tensor contribution. Thus, attempts have never been devoted, until very recently, to study the effects of the tensor force on the evolution of the shell structure of atomic nuclei.

In Ref. [6] it has been pointed out that the tensor force provides a specific attraction (repulsion) between $j_>$ and $j_<$ ($j_>$ and $j_>$, or $j_<$ and $j_<$) single-nucleon orbitals with different isospin. These tensor correlations were found to have strong impact on the evolution of the shell structure as a function of neutron or proton excess. In the framework of mean-field calculations the issue has been addressed in Ref. [7] using the Gogny interaction and in Ref. [8] using the Skyrme interaction. We would like to point out that the effects of the tensor force can be understood in a very transparent way by inspecting the Skyrme Hartree-Fock (SHF), or SHF plus Baardeen-Cooper-Schrieffer (SHF+BCS), formulas. In Ref. [9], the detailed study of the Sn isotopes, and $N = 82$ isotones, has been performed taking into account the effects of the triplet-even and triplet-odd tensor contributions separately. The effect of the tensor force on the evolution of single-particle states was analyzed by other groups as well [10–12].

In the present paper, which is a follow-up of Ref. [9], we extend our study of the tensor correlations to lighter systems. The goal is to see whether the same conclusions reached before, can be confirmed by looking at empirical data in another mass region. The work has been in particular motivated by the recent experimental work reported in Ref. [13], where data on the evolution of the levels in the fp-shell in unstable systems have been extracted from transfer reactions.

The outline of the paper is as follows. The theoretical framework of SHF plus BCS is described briefly in Sec. II. In Sec. III, the isospin dependence of the the spin-orbit splittings in the Ca isotopes and the $N = 28$ isotones is presented, and the discussion is then focused on the behavior of f and p orbitals in the ^{48}Ca and ^{46}Ar nuclei. Finally, we draw conclusions in Sec. IV.

II. THEORETICAL FRAMEWORK

The triplet-even and triplet-odd zero-range tensor terms read

$$\begin{aligned} v_T = \frac{T}{2}\Bigg\{&\left[(\boldsymbol{\sigma}_1\cdot\boldsymbol{k}')(\boldsymbol{\sigma}_2\cdot\boldsymbol{k}') - \frac{1}{3}\boldsymbol{k}'^2(\boldsymbol{\sigma}_1\cdot\boldsymbol{\sigma}_2)\right]\delta(\boldsymbol{r}_1-\boldsymbol{r}_2)\\ &+\left[(\boldsymbol{\sigma}_1\cdot\boldsymbol{k})(\boldsymbol{\sigma}_2\cdot\boldsymbol{k}) - \frac{1}{3}(\boldsymbol{\sigma}_1\cdot\boldsymbol{\sigma}_2)\boldsymbol{k}^2\right]\delta(\boldsymbol{r}_1-\boldsymbol{r}_2)\Bigg\}\\ &+U\Bigg\{(\boldsymbol{\sigma}_1\cdot\boldsymbol{k}')\delta(\boldsymbol{r}_1-\boldsymbol{r}_2)(\boldsymbol{\sigma}_2\cdot\boldsymbol{k})\\ &-\frac{1}{3}(\boldsymbol{\sigma}_1\cdot\boldsymbol{\sigma}_2)[\boldsymbol{k}'\cdot\delta(\boldsymbol{r}_1-\boldsymbol{r}_2)\boldsymbol{k}]\Bigg\}. \end{aligned} \tag{1}$$

In the above expression, the operator $\boldsymbol{k} = (\nabla_1 - \nabla_2)/2i$ acts on the right, and $\boldsymbol{k}' = -(\nabla_1 - \nabla_2)/2i$ acts on the left. The coupling constants T and U denote the strength of the triplet-even and triplet-odd tensor interactions, respectively. In Ref. [9], optimal values of these parameters have been extracted by comparing the results for the single-particle states along the $Z = 50$ isotopes and $N = 82$ isotones with the

experimental data [14]. We will use the same parameters in the present work.

The tensor interactions in Eq. (1) give contributions both to the binding energy and to the spin-orbit splitting, which are, respectively, quadratic and linear in the proton and neutron spin-orbit densities,

$$J_q(r) = \frac{1}{4\pi r^3}\sum_i v_i^2(2j_i+1)\left[j_i(j_i+1) - l_i(l_i+1) - \frac{3}{4}\right] \times R_i^2(r). \quad (2)$$

The isospin quantum number $q = 0(1)$ labels neutrons (proton) and $i = n, l, j$ runs over all states having the given q. The quantity v_i^2 is the BCS occupation probability of each orbital and $R_i(r) \equiv \frac{u_i(r)}{r}$ is the radial part of the wave function. The spin-orbit density J_q has a peculiar behavior, since it gives negligibly small contributions in the spin-saturated cases, but it increases linearly with the number of particles if only one of the spin-orbit partners is filled. The sign of J_q will change depending upon the quantum numbers of the orbitals which are progressively filled: that is, the orbital with $j_>$ gives a positive contribution to J_q while the orbital with $j_<$ gives a negative contribution to J_q.

It should be also noticed that the exchange part of the central Skyrme interaction gives the same kind of contribution to the total energy density and spin-orbit splitting. The central exchange and tensor contributions to the energy density which depend on the spin-orbit densities, $\mathscr{H}_{\text{central+tensor}}$, are

$$\mathscr{H}_{\text{central+tensor}} = \tfrac{1}{2}\alpha\left(J_n^2 + J_p^2\right) + \beta J_n J_p. \quad (3)$$

The spin-orbit potential is then given by

$$U_{s.o.}^{(q)} = \frac{1}{2r}\left(2W_0\frac{d\rho_q}{dr} + W_0'\frac{d\rho_{q'}}{dr}\right) + \left(\alpha\frac{J_q}{r} + \beta\frac{J_{q'}}{r}\right). \quad (4)$$

The terms in the first bracket on the right-hand side (rhs) comes from the Skyrme spin-orbit interaction. We should notice that for most of the Skyrme parameter sets $W_0 = W_0'$. The parameter sets with values $W_0 \neq W_0'$ have been introduced in [15]. In all the parameter sets, W_0 is always taken to be positive, whereas the radial derivatives of the densities are mostly negative. The terms in the second brackets in Eq. (4) includes both the central exchange and the tensor contributions, that is, $\alpha = \alpha_C + \alpha_T$ and $\beta = \beta_C + \beta_T$. The central exchange contributions are written in terms of the usual Skyrme parameters,

$$\begin{aligned}\alpha_C &= \tfrac{1}{8}(t_1 - t_2) - \tfrac{1}{8}(t_1x_1 + t_2x_2),\\ \beta_C &= -\tfrac{1}{8}(t_1x_1 + t_2x_2),\end{aligned} \quad (5)$$

while the tensor contributions are expressed as

$$\begin{aligned}\alpha_T &= \tfrac{5}{12}U,\\ \beta_T &= \tfrac{5}{24}(T+U).\end{aligned} \quad (6)$$

The parameters employed in the present work are the same as those of Ref. [9]: $\alpha_T = -170$ MeV fm^5 and $\beta_T = 100$ MeV fm^5. We combine this tensor force with the Skyrme force SLy5 [16] for which $\alpha_C = 80.2$ MeV fm^5 and $\beta_C = -48.9$ MeV fm^5. Consequently, we get $\alpha = -88.8$ MeV fm^5 and $\beta = 51.1$ MeV fm^5.

Except for the double-magic systems, we perform HF-BCS in order to take into account the pairing correlations. There is an ongoing debate whether pairing in nuclei is concentrated preferentially in the bulk or at the surface (cf., e.g., Ref. [17]). Therefore, for the pairing interaction we use either a pure δ force (DF) or a density-dependent δ interaction (DDDI). In the former case, we write

$$V = V_0\delta(\boldsymbol{r}_1 - \boldsymbol{r}_2) \quad (7)$$

and in the latter,

$$V = V_0\left(1 - x\left(\frac{\rho(\frac{r_1+r_2}{2})}{\rho_0}\right)^\gamma\right)\cdot\delta(\boldsymbol{r}_1 - \boldsymbol{r}_2), \quad (8)$$

keeping fixed $x = 1, \gamma = 1$ and $\rho_0 = 0.16$ fm^{-3}. In both cases V_0 is a free parameter which should be determined by comparing the pairing gaps obtained within BCS either using the DF or the DDDI, with the empirical values.

Following Ref. [18], we determine the empirical pairing gap from the five-point formula,

$$\begin{aligned}\triangle_n^{(5)}(N) = -\frac{(-1)^N}{8}[&E(N+2) - 4E(N+1)\\ &+ 6E(N) - 4E(N-1) + E(N-2)],\end{aligned} \quad (9)$$

to compare it with an averaged calculated gap of the states around the Fermi surface. We extract also another empirical pairing gap from the three-point formula,

$$\triangle_n^{(3)}(N) = \frac{(-1)^N}{2}[E(N-1) - 2E(N) + E(N+1)], \quad (10)$$

to compare it with the calculated maximum pairing gap at the Fermi surface. In the above formulas, N is the neutron number and E is the total binding energy. If we wish to study an isotone chain we can use for protons equivalent formulas, by replacing N by Z in Eqs. (9) and (10).

As far as the results being discussed in Sec. III are concerned, we have verified that only small variations are produced if the calculations are performed without pairing, by using the DF or the DDDI.

III. RESULTS

A. The spin-orbit splittings in the Ca isotopes and in the $N = 28$ isotones

The HF+BCS calculations are performed for Ca isotopes by using the Skyrme interaction SLy5 [16] and two different pairing interactions. The calculated pairing gaps of $1f_{7/2}$orbit ($\Delta_n(f_{7/2})$), and the average pairing gap are shown in Fig. 1 in comparison with the empirical neutron pairing gaps obtained by the three-point and five-point formulas, respectively. As an optimal suitable parameter we get $V_0 = 740$ MeV fm^3 in the case of the density dependent δ-interaction (DDDI) and $V_0 = 305$ MeV fm^3 for the δ-force (DF).

In Fig. 2, the energy differences between the $1d_{3/2}$ and the $2s_{1/2}$ proton states and between the $1d_{3/2}$ and the $1d_{5/2}$ proton states in the Ca isotopes, are shown as a function of the mass number A. The SLy5 interaction without tensor terms fails to reproduce the trend of the experimental data.

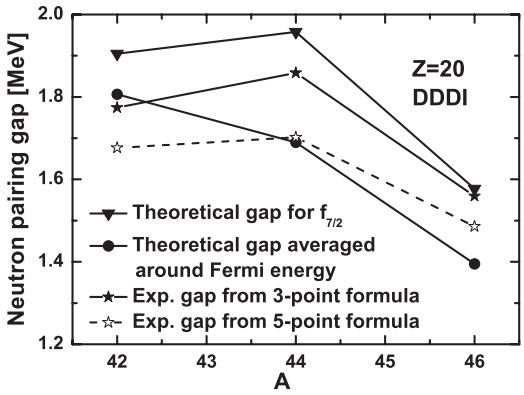

FIG. 1. Theoretical neutron pairing gaps for the Ca isotopes obtained by using HF-BCS, with SLy5 plus the density-dependent δ interaction (DDDI). The comparison with the empirical values (see the text for a short discussion about the two empirical formulas) allows fitting the parameter $V_0 = 740$ MeV fm^3.

One can notice a substantial improvement by including the tensor terms and using the same parameters already employed for Sn and the $N = 82$ isotones in Ref. [9], i.e., $\alpha_T = -170$ MeV fm^5 and $\beta_T = 100$ MeV fm^5. In particular, the experimental results in the magic nuclei ^{40}Ca and ^{48}Ca are reproduced in a satisfactory way. These results can be qualitatively understood in terms of the arguments drawn from Eq. (4). The Ca isotopes are spin-saturated nuclei as far as the protons are concerned so that the proton spin density J_p is negligibly small and the term with α in the spin-orbit potential does not give any appreciable contribution. On the other hand, J_n is finite and the term with β is responsible for the isospin dependence of the spin-orbit splitting. From $A = 42$ to $A = 48$, the $f_{7/2}$ neutron orbit is gradually filled and the positive J_n is increased. Then, the positive value of β_T shrinks in absolute value the spin-orbit potential and decreases the spin-orbit splitting [one should notice that the terms in the first bracket in the rhs of Eq. (4) give negative contribution]. This mechanism explains why the energy differences between the $1d_{3/2}$ and the $1d_{5/2}$ or $2s_{1/2}$ states decrease in Fig. 2, when the tensor force is included. Without the tensor terms, the trend of the spin-orbit splitting is opposite to the experiment. We should also remark that the energy difference varies as a straight line in Fig. 2, while the experimental data show a kink at $A = 44$. This kind of nonmonotonic isotopic effect might be due to correlations beyond mean field, like the coupling with low-lying vibrations [20].

We get the experimental data in Fig. 2 from the $(d,{}^3\mathrm{He})$ experiment reported in Ref. [19]. In the experimental spectra, for every (l, j) value, the spectroscopic strength is to some extent fragmented in different peaks. The DWBA analysis allows the extraction of spectroscopic factors C^2S associated to each peak. We have extracted from experimental data the centroid energies for each (l, j),

$$\overline{E_x} = \frac{\sum_i (E_x)_i (C^2S)_i}{\sum_i (C^2S)_i}, \tag{11}$$

where the sum runs over the peaks which are experimentally identified. This average has been adopted in Fig. 2 and also in Ref. [21] and in Fig. 4 of Ref. [22]. If only the lowest state of the $\frac{1}{2}^+$ distribution is considered, instead of the centroid, like in Refs. [12,23], one finds an inversion between the $1d_{3/2}$ and $2s_{1/2}$ proton levels in ^{48}Ca. However, in order to compare with the mean field results, the averaged value (11) looks more appropriate to refer as the empirical value.

In order to further study the effects of the tensor force on single-particle states, we also examine the evolution of the spin-orbit splitting along the $N = 28$ isotones. The calculated results are shown in Fig. 3 together with available experimental data in ^{44}S and ^{48}Ca. We can see a large quenching of the spin-orbit splitting between $1d$-orbits for $A = 48$. We can, once more, understand this quenching by inspecting Eq. (4). Along the isotone chain considered, the proton $1d_{3/2}$ state is gradually filled, and this gives a negative contribution to the proton spin-orbit density J_p. Because of the negative value of α_T, the spin-orbit potential for protons in Eq. (4) is reduced in absolute value, and the spin-orbit splitting decreases. For

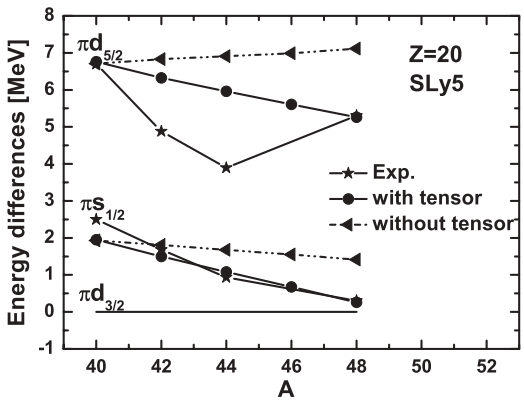

FIG. 2. Energy differences between the $1d_{3/2}$ single-proton state and, respectively, the $2s_{1/2}$ and $1d_{5/2}$ states, plotted along the Ca isotopes. The calculations are performed within HF-BCS, using SLy5 and the DDDI for pairing, without and with the tensor terms. The experimental data are taken from Ref. [19].

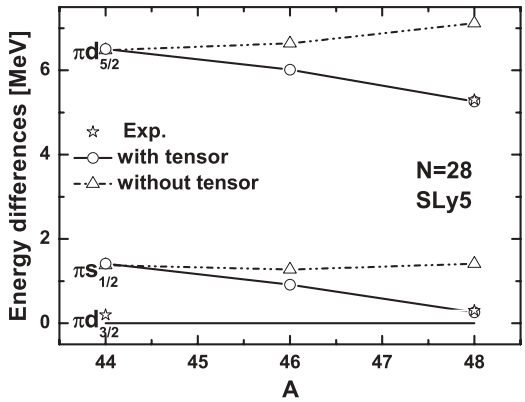

FIG. 3. Energy differences between the $1d_{3/2}$ single-proton state and, respectively, the $2s_{1/2}$ and $1d_{5/2}$ states, plotted for the $N = 28$ isotones. The calculations are performed within HF-BCS, using SLy5 and the DDDI for pairing, without and with the tensor terms. The experimental data are taken from Ref. [19].

the $N = 28$ isotones, the spin-orbit density J_n is not changed so that β_T does not play any role in these nuclei. While the choice of negative α_T works certainly in the $N = 28$ isotones, we need more data to confirm the conclusion on the value of α_T.

We have then studied the neutron states in the Ca isotopes, by defining the same quantity δ^{Ca} already introduced by the authors of [12], namely,

$$\delta^{\mathrm{Ca}} = \left(\varepsilon_{\nu 1d_{3/2}}(^{48}\mathrm{Ca}) - \varepsilon_{\nu 2s_{1/2}}(^{48}\mathrm{Ca})\right) - \left(\varepsilon_{\nu 1d_{3/2}}(^{40}\mathrm{Ca}) - \varepsilon_{\nu 2s_{1/2}}(^{40}\mathrm{Ca})\right). \quad (12)$$

Whereas the experimental value for this quantity is about -2.2 MeV, we obtain $+0.2$ MeV with our optimal α and β values. It was pointed out in Ref. [12] that the positive α_T is necessary to get better agreement with the experimental trend.

B. The reduction of the neutron spin-orbit splittings in going from ^{48}Ca to ^{46}Ar

Let us now discuss the neutron spin-orbit splittings of $2p$ and $1f$ orbits in ^{48}Ca to ^{46}Ar (see also [24]). This problem is intimately connected to that of the evolution of $N = 28$ shell gap from ^{48}Ca to ^{46}Ar. Figure 4 displays the single-neutron energies of the f- and p-orbits for ^{48}Ca and ^{46}Ar. We compare the experimental data with the results obtained by employing the force SLy5 without and with the tensor contribution. In connection with the experimental data, we should stress that the peaks which were clearly identified in Ref. [13] do not exhaust the full spectroscopic strength and some missing fragments have been taken from shell-model calculations in order to extract the numbers which we quote in Table I (see also the discussion in [25]). In our calculations, one can see from the Table that the f and p spin-orbit splittings have been reduced by 0.49 MeV and 0.28 MeV, respectively, between ^{48}Ca and ^{46}Ar, when the tensor terms are included. If the tensor terms are not included, the variation between ^{48}Ca and ^{46}Ar has opposite sign to the experimental finding. We should

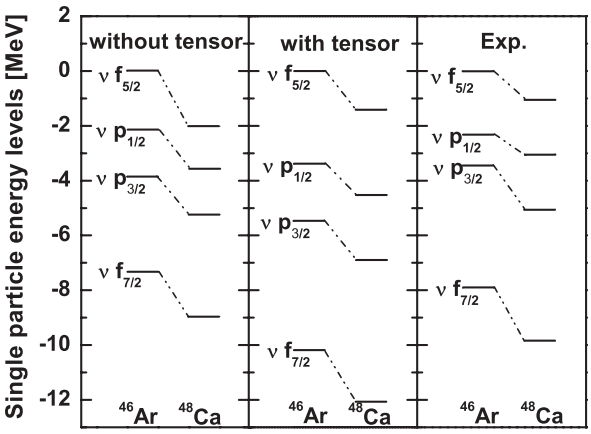

FIG. 4. Neutron single-particle energies of the f- and p-orbits in ^{48}Ca and ^{46}Ar. The Skyrme parametrization SLy5 is employed here as in the other cases. We compare in the three panels calculations without and with the tensor terms, and experimental data taken from Ref. [13].

TABLE I. In the first two parts, the spin-orbit splittings for the f and p orbits respectively, ΔE_f and ΔE_p, are displayed. We show the values in ^{48}Ca and ^{46}Ar, as well as their difference. In the last part we display instead the value of the $N = 28$ shell gap, namely $\Delta E_{\mathrm{gap}} \equiv \varepsilon(p_{3/2}) - \varepsilon(f_{7/2})$. In all cases, the theoretical results are obtained by using the Skyrme force SLy5, with and without the tensor terms.

		SLy5	
	Exp. [13]	with tensor	w/o tensor
$\Delta E_f(^{48}\mathrm{Ca})$	8.80	10.68	6.94
$\Delta E_f(^{46}\mathrm{Ar})$	7.92	10.19	7.32
$\Delta E_f(^{48}\mathrm{Ca}) - \Delta E_f(^{46}\mathrm{Ar})$	0.88	0.49	−0.38
$\Delta E_p(^{48}\mathrm{Ca})$	2.02	2.36	1.68
$\Delta E_p(^{46}\mathrm{Ar})$	1.13	2.08	1.72
$\Delta E_p(^{48}\mathrm{Ca}) - \Delta E_p(^{46}\mathrm{Ar})$	0.89	0.28	−0.04
$\Delta E_{\mathrm{gap}}(^{48}\mathrm{Ca})$	4.80	5.16	3.71
$\Delta E_{\mathrm{gap}}(^{46}\mathrm{Ar})$	4.47	4.71	3.46
$\Delta E_{\mathrm{gap}}(^{48}\mathrm{Ca}) - \Delta E_{\mathrm{gap}}(^{46}\mathrm{Ar})$	0.33	0.45	0.25

notice that the shell-model calculations in Ref. [25], which take properly into account the correlation effects, give much smaller reduction of the empirical spin-orbit splittings than that listed in Table I and provide a better agreement between the experiment and the present result. We find also that the tensor force makes the reduction of the $N = 28$ gap larger.

We can interpret our results in the following way. The variation of the spin-orbit splitting of f-orbits from ^{48}Ca to ^{46}Ar is produced by the variations of $\frac{d\rho_p}{dr}$ and J_p [cf. Eq. (4)]. The two protons can be removed either from the $d_{3/2}$ or the $s_{1/2}$ orbit, according to the energy position of the two levels and the magnitude of the pairing force. In the present calculation we find that most of the change is associated with a depletion of the d orbit. The effect of this proton depletion on the spin-orbit splitting of the νf orbit is given by two terms, namely,

$$\frac{W_0}{2}\int dr\,\frac{u^2_{\nu f7/2}}{r}\left[\frac{d\rho_p}{dr}(^{48}\mathrm{Ca}) - \frac{d\rho_p}{dr}(^{46}\mathrm{Ar})\right] \quad (13)$$

and

$$\beta\int dr\,\frac{u^2_{\nu f7/2}}{r}\left[J_p(^{48}\mathrm{Ca}) - J_p(^{46}\mathrm{Ar})\right]. \quad (14)$$

In Fig. 5 we plot the relevant quantities for the present analysis. In the region where the wave functions of the f orbits are large, both the difference between the derivatives of the proton densities in the two isotopes and that between the spin-orbit densities, are mainly negative. Without tensor, since W_0 is positive and $\beta = \beta_C$ is negative, the contribution (13) tends to decrease the spin-orbit splitting whereas the contribution (14) tends to increase it. The latter contribution turns out to be numerically larger than the former one, so that in Table I one can notice a small increase of the splitting. In the case of the p orbits, the increase is smaller, in keeping with the fact that there exists a small region where the quantity $[\frac{d\rho_p}{dr}(^{48}\mathrm{Ca}) - \frac{d\rho_p}{dr}(^{46}\mathrm{Ar})]$ is positive. Therefore, the calculation without the tensor force point to an increase of the spin-orbit splitting

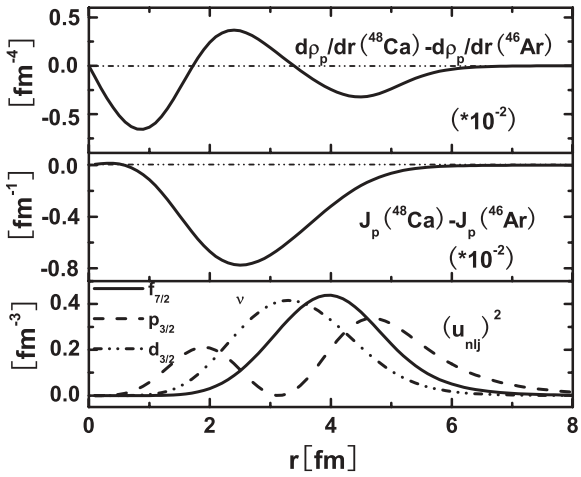

FIG. 5. Upper panel: difference between $\frac{d\rho_p}{dr}$ in ^{48}Ca and ^{46}Ar. Middle panel: difference between J_p in ^{48}Ca and ^{46}Ar. Lower panel: square of the wave functions of the neutron states, which is another contribution to the integrand of Eqs. (13) and (14). See the text for a discussion.

between ^{48}Ca and ^{46}Ar, and cannot explain the experimental reduction. When the tensor force is taken into account, both contributions (13) and (14) produce a reduction of the spin-orbit splitting because $\beta = \beta_C + \beta_T$ is now positive.

In Table I we also show that the tensor interaction produces a sizable variation of the $N = 28$ shell gap. This is explained by the larger variation of the spin-orbit splitting for the f orbits, as compared with the p orbits. The result can be understood also in terms of the argument made in the Introduction: the tensor interaction between $\nu j_>$ and $\pi j_<$ ($\nu j_<$ and $\pi j_<$) is attractive (repulsive), so that the removal of two protons from $\pi d_{3/2}$ should reduce the spin-orbit splitting of νf and p orbits and consequently the size of the $N = 28$ gap. From our numerical results, we confirm that the effect of the tensor terms is important.

IV. SUMMARY

In summary, we have demonstrated that the addition of the tensor terms can fairly well explain the trend of the proton single-particle states along the Ca isotopes, with the same parameters already used in Ref. [9]. At the same time, we are able to explain qualitatively the reduction of the neutron spin-orbin splittings from ^{48}Ca to ^{46}Ar as an effect of the tensor force (without the tensor, we would have instead an increase of the spin-orbit splitting). These two examples show the important role of the proton-neutron tensor interaction both in medium-mass and in heavy nuclei, governed by β_T within our framework. On the other hand, proton states along the $N = 28$ isotones and neutron states in the Ca isotopes are not so well understood, raising questions about our choice of the sign of the proton-proton or neutron-neutron tensor interaction associated with α_T.

The aim of the present paper is to show more results from the perturbative approach, in a different mass region compared to our previous work [9]. In Ref. [12], on the other hand, new Skyrme parameter sets are fitted after choosing a definite strength of the tensor components. In certain cases (like for the proton states in the Ca isotopes), our results obtained by adding the tensor force perturbatively show better agreement with the experimental findings than those obtained in Ref. [12], whereas in other cases this is not true.

In all the recent works devoted to the single-particle states the particle-vibration coupling is mentioned but not taken into account so far within the same framework. A serious step forward in this direction has to be made.

ACKNOWLEDGMENTS

We acknowledge the financial support from the the Asia-Link project [CN/ASIA-LINK/008(94791)] of the European Commission. The work is also partly supported by the National Natural Science Foundation of China under contract nos. 10475116, 10775183 and Major State Basic Research Development Program in China under contract no. 2007CB815000.

[1] T. H. R. Skyrme, Philos. Mag. **1**, 1043 (1956); J. S. Bell and T. H. R. Skyrme, *ibid*. **1**, 1055 (1956); T. H. R. Skyrme, Nucl. Phys. **9**, 615 (1958); **9**, 635 (1958).
[2] D. Vautherin and D. M. Brink, Phys. Rev. C **5**, 626 (1972); M. Beiner, H. Flocard, N. Van Giai, and P. Quentin, Nucl. Phys. **A238**, 29 (1975).
[3] F. Stancu, D. M. Brink, and H. Flocard, Phys. Lett. **B68**, 108 (1977).
[4] F. Tondeur, Phys. Lett. **B123**, 139 (1983).
[5] K. F. Liu *et al*., Nucl. Phys. **A534**, 1 (1991); **A534**, 25 (1991); **A534**, 48 (1991).
[6] T. Otsuka, T. Suzuki, R. Fujimoto, H. Grawe, and Y. Akaishi, Phys. Rev. Lett. **95**, 232502 (2005).
[7] T. Otsuka, T. Matsuo, and D. Abe, Phys. Rev. Lett. **97**, 162501 (2006).
[8] B. A. Brown, T. Duguet, T. Otsuka, D. Abe, and T. Suzuki, Phys. Rev. C **74**, 061303(R) (2006).
[9] G. Colò, H. Sagawa, S. Fracasso, and P. F. Bortignon, Phys. Lett. **B646**, 227 (2007).
[10] D. M. Brink and F. Stancu, Phys. Rev. C **75**, 064311 (2007).
[11] J. Dobaczewski, in *Proceedings of the Third ANL/MSU/JINA/INT RIA Workshop,* edited by T. Duguet, H. Esbensen, K. M. Nollett, and C. D. Roberts (World Scientific, Singapore, 2006).
[12] T. Lesinski, M. Bender, K. Bennaceur, T. Duguet, and J. Meyer, Phys. Rev. C **76**, 014312 (2007).
[13] L. Gaudefroy *et al*., Phys. Rev. Lett. **97**, 092501 (2006).
[14] J. P. Schiffer *et al*., Phys. Rev. Lett. **92**, 162501 (2004).
[15] P.-G. Reinhard and H. Flocard, Nucl. Phys. **A584**, 467 (1995).
[16] E. Chabanat, P. Bonche, P. Haensel, J. Meyer, and R. Schaeffer, Nucl. Phys. **A635**, 231 (1998).
[17] N. Sandulescu, P. Schuck, and X. Viñas, Phys. Rev. C **71**, 054303 (2005).
[18] M. Bender, K. Rutz, P.-G. Reinhard, and J. A. Maruhn, Eur. Phys. J. A **8**, 59 (2000).
[19] P. Doll, G. J. Wagner, and K. T. Knopfle, Nucl. Phys. **A263**, 270 (1976).
[20] C. Mahaux, P. F. Bortignon, R. A. Broglia, and C. H. Dasso, Phys. Rep. **120**, 1 (1985).

[21] P. D. Cottle and K. W. Kemper, Phys. Rev. C **58**, 3761 (1998).
[22] J. Fridmann *et al*., Nature (London) **435**, 922 (2005).
[23] M. Grasso, Z.-Y. Ma, E. Khan, J. Margueron, and N. Van Giai, Phys. Rev. C **76**, 044319 (2007).
[24] B. G. Todd-Rutel, J. Piekarewicz, and P. D. Cottle, Phys. Rev. C **69**, 021301(R) (2004).
[25] A. Signoracci and B. A. Brown, Phys. Rev. Lett. **99**, 099201 (2007); L. Gaudefroy *et al*., *ibid*. **99**, 099202 (2007).